ORTHOGONAL SERIES ESTIMATION OF THE PAIR CORRELATION FUNCTION OF A SPATIAL POINT PROCESS

Abdollah Jalilian[1], Yongtao Guan[2] and Rasmus Waagepetersen[3]

[1]*Razi University,* [2]*University of Miami and* [3]*Aalborg University*

Supplementary Material

S1 Expanding observation window

This section states a few results on the asymptotic behavior of the edge correction $e_n(h)$ (defined in (4.9) in the main document) and related ratios. For each $n \geq 1$ and $h, h_1, h_2 \in \mathbb{R}^d$,

$$|W_n \cap (W_n)_h| = \begin{cases} \prod_{i=1}^d (2na_i - |h_i|) & |h_i| < 2na_i, i = 1, \ldots, d \\ 0 & \text{otherwise} \end{cases}$$

and

$$\left|W_n \cap (W_n)_{h_1} \cap (W_n)_{h_2}\right| = \begin{cases} V_n(h_1, h_2) & \max\{|h_{1i}|, |h_{2,i}|, |h_{1i} - h_{2i}|\} < 2na_i, i = 1, \ldots, d \\ 0 & \text{otherwise} \end{cases}$$

where $V_n(h_1, h_2) = \prod_{i=1}^d \big(2na_i - \max\{0, h_{1i}, h_{2i}\} + \min\{0, h_{1i}, h_{2i}\}\big)$. Therefore, for any fixed $h, h_1, h_2 \in \mathbb{R}^d$, as $n \to \infty$,

$$e_n(h) = \frac{|W_n \cap (W_n)_h|}{|W_n|} = \prod_{i=1}^d \left(1 - \frac{|h_i|}{2na_i}\right) \to 1. \tag{S1.1}$$

If $n \geq R/\min_{1\leq i\leq d} a_i$ or equivalently $B^R_{r_{\min}} \subset W_n$, then $1/2^d \leq e_n(h) \leq 1$ for any $h \in B^R_{r_{\min}}$.

Further,

$$\frac{\big|W_n \cap (W_n)_{h_1} \cap (W_n)_{h_2}\big|}{|W_n|} = \prod_{i=1}^d \left(1 - \frac{\max\{0, h_{1i}, h_{2i}\} - \min\{0, h_{1i}, h_{2i}\}}{2na_i}\right) \to 1. \tag{S1.2}$$

Similarly, it can be shown that for any fixed $h_1, h_2, h_3 \in \mathbb{R}^d$,

$$\big|W_n \cap (W_n)_{h_1} \cap (W_n)_{h_3} \cap (W_n)_{h_2+h_3}\big|/|W_n| \to 1.$$

S2 Proofs

S2.1 Proof of Lemma 1

For n large enough, $\mathbb{I}(h \in B^R_{r_{\min}}) > 0$ implies $|W_n \cap (W_n)_h| > 0$. Then, by the second order Campbell formula (see Møller and Waagepetersen, 2003, Section C.2.1),

$$\begin{aligned}\mathbb{E}(\hat{\theta}_{k,n}) =& \frac{1}{\varsigma_d |W_n|}\int_{W_n^2} \frac{\phi_k(\|v-u\|-r_{\min})w(\|v-u\|-r_{\min})}{\|v-u\|^{d-1}e_n(v-u)} \\ & \qquad \mathbb{I}(v-u\in B^R_{r_{\min}})g(\|v-u\|)\mathrm{d}u\mathrm{d}v \\ =& \int_{\mathbb{R}^d}\frac{g(\|h\|)\phi_k(\|h\|-r_{\min})w(\|h\|-r_{\min})}{\varsigma_d\|h\|^{d-1}} \\ & \qquad \mathbb{I}(h\in B^R_{r_{\min}})\left(\int_{\mathbb{R}^d}\frac{\mathbb{I}\{v\in W_n\cap (W_n)_h\}}{|W_n\cap (W_n)_h|}\mathrm{d}v\right)\mathrm{d}h \\ =& \int_{r_{\min}}^{r_{\min}+R} g(r)\phi_k(r-r_{\min})w(r-r_{\min})\mathrm{d}r=\theta_k.\end{aligned}$$

Let $f_k(h)=\phi_k(\|h\|-r_{\min})w(\|h\|-r_{\min})/\|h\|^{d-1}$. Then, by the second to fourth order Campbell formulae (omitting the details),

$$\begin{aligned}\mathbb{V}\mathrm{ar}(\hat{\theta}_{k,n}) =& \frac{1}{\varsigma_d{}^2|W_n|}\Bigg[2\int_{B^R_{r_{\min}}} g(h)f_k^2(\|h\|)G_n^{(2)}(h)\mathrm{d}h \\ & + 4\int_{B^R_{r_{\min}}}\int_{B^R_{r_{\min}}} g^{(3)}(h_1,h_2)f_k(\|h_1\|)f_k(\|h_2\|)G_n^{(3)}(h_1,h_2)\mathrm{d}h_1\mathrm{d}h_2 \\ & + \int_{B^R_{r_{\min}}}\int_{B^R_{r_{\min}}} f_k(\|h_1\|)f_k(\|h_2\|)G_n^{(4)}(h_1,h_2)\mathrm{d}h_1\mathrm{d}h_2\Bigg],\end{aligned} \tag{S2.3}$$

where

$$\begin{aligned}G_n^{(2)}(h) &= \frac{1}{e_n^2(h)}\left[\frac{1}{|W_n|}\int_{W_n}\frac{\mathbf{1}[u+h\in W_n]}{\rho(u)\rho(u+h)}\mathrm{d}u\right], \\ G_n^{(3)}(h_1,h_2) &= \frac{1}{e_n(h_1)e_n(h_2)}\left[\frac{1}{|W_n|}\int_{W_n}\frac{\mathbf{1}[u\in (W_n)_{h_1}\cap (W_n)_{h_2}]}{\rho(u)}\mathrm{d}u\right], \\ G_n^{(4)}(h_1,h_2) &= \frac{1}{e_n(h_1)e_n(h_2)}\int_{\mathbb{R}^2}\left[g^{(4)}(h_1,u,h_2+u)-g(h_1)g(h_2)\right] \\ & \qquad \frac{\left|W_n\cap (W_n)_u\cap (W_n)_{h_1}\cap (W_n)_{h_2}\right|}{|W_n|}\mathrm{d}u.\end{aligned}$$

For $n \geq R/\min_{1\leq i\leq d} a_i$ and any $h, h_1, h_2 \in B^R_{r_{\min}}$, by V1 and Section S1,

$$\begin{aligned} G^{(2)}_n(h) &= \frac{1}{e^2_n(h)}\left[\frac{1}{|W_n|}\int_{W_n}\frac{\mathbf{1}[u+h\in W_n]}{\rho(u)\rho(u+h)}\mathrm{d}u\right] \leq \frac{1}{\rho^2_{\min}e_n(h)} \leq \frac{2^d}{\rho^2_{\min}}, \\ G^{(3)}_n(h_1,h_2) &= \frac{1}{e_n(h_1)e_n(h_2)}\left[\frac{1}{|W_n|}\int_{W_n}\frac{\mathbf{1}[u\in (W_n)_{h_1}\cap (W_n)_{h_2}]}{\rho(u)}\mathrm{d}u\right] \\ &\leq \frac{1}{\rho_{\min}e_n(h)} \leq \frac{2^d}{\rho_{\min}} \end{aligned}$$

and by V3,

$$\begin{aligned} \left|G^{(4)}_n(h_1,h_2)\right| &\leq \frac{1}{e_n(h_1)e_n(h_2)}\int_{\mathbb{R}^2}\left|g^{(4)}(h_1,u,h_2+u)-g(h_1)g(h_2)\right| \\ &\qquad\qquad \frac{\left|W_n\cap (W_n)_u\cap (W_n)_{h_1}\cap (W_n)_{h_2}\right|}{|W_n|}\mathrm{d}u \\ &\leq \frac{1}{e_n(h_1)}\int_{\mathbb{R}^2}\left|g^{(4)}(h_1,u,h_2+u)-g(h_1)g(h_2)\right|\mathrm{d}u \\ &\leq 2^d\int_{\mathbb{R}^2}\left|g^{(4)}(h_1,u,h_2+u)-g(h_1)g(h_2)\right|\mathrm{d}u \leq 2^dC_4. \end{aligned}$$

Thus, using V2, for all $k\geq 1$ and $n \geq R/\min_{1\leq i\leq d} a_i$,

$$\begin{aligned} \mathbb{V}\mathrm{ar}(\hat{\theta}_{k,n}) \leq \frac{1}{\varsigma_d{}^2|W_n|}\Bigg[&\frac{2^{d+1}}{\rho^2_{\min}}\int_{B^R_{r_{\min}}} f^2_k(\|h\|)g(\|h\|)\mathrm{d}h \\ &+ \frac{2^{d+2}}{\rho_{\min}}C_3\left(\int_{B^R_{r_{\min}}}\left|f_k(\|h\|)\right|\mathrm{d}h\right)^2 \\ &+ 2^dC_4\left(\int_{B^R_{r_{\min}}}\left|f_k(\|h\|)\right|\mathrm{d}h\right)^2\Bigg]. \end{aligned}$$

But for all $k \geq 1$,

$$\begin{aligned}
\int_{B_{r_{\min}}^R} f_k^2(\|h\|)g(\|h\|)\mathrm{d}h &= \int_{r_{\min}}^{r_{\min}+R} \phi_k^2(r - r_{\min})g(r)\frac{w^2(r - r_{\min})}{r^{d-1}}\mathrm{d}r \\
&= \int_0^R \phi_k^2(r)g(r + r_{\min})\frac{w^2(r)}{(r + r_{\min})^{d-1}}\mathrm{d}r \\
&\leq C_2 \int_0^R \phi_k^2(r)w(r)\mathrm{d}r = C_2,
\end{aligned}$$

and by Hölder's inequality,

$$\begin{aligned}
\int_{B_{r_{\min}}^R} \left|f_k(\|h\|)\right|\mathrm{d}h &= \int_{B_{r_{\min}}^R} \left|\phi_k(\|h\| - r_{\min})\right|\frac{w(\|h\| - r_{\min})}{\|h\|^{d-1}}\mathrm{d}h \\
&= \int_{r_{\min}}^{r_{\min}+R} \left|\phi_k(r - r_{\min})\right|w(r - r_{\min})\mathrm{d}r \\
&\leq \left(\int_0^R \phi_k^2(r)w(r)\mathrm{d}r\right)^{1/2} \left(\int_0^R w(r)\mathrm{d}r\right)^{1/2} \\
&= \left(\int_0^R w(r)\mathrm{d}r\right)^{1/2} < \infty.
\end{aligned}$$

Therefore

$$\mathbb{V}\mathrm{ar}(\hat{\theta}_{k,n}) < \frac{1}{\varsigma_d{}^2|W_n|}\left[\frac{2^{d+1}}{\rho_{\min}^2}C_2 + \left(\frac{2^{d+2}}{\rho_{\min}}C_3 + 2^dC_4\right)\left(\int_0^R w(r)\mathrm{d}r\right)\right] = \frac{C_1}{|W_n|},$$

where

$$C_1 = \frac{1}{\varsigma_d{}^2}\left[\frac{2^{d+1}}{\rho_{\min}^2}C_2 + \left(\frac{2^{d+2}}{\rho_{\min}}C_3 + 2^dC_4\right)\left(\int_0^R w(r)\mathrm{d}r\right)\right] > 0.$$

S2.2 Proof of Lemma 2

Consider a real function f on $\mathbb{R}^d \times \mathbb{R}^d$ where $f(h_1, h_2) \neq 0$ implies $|W_n \cap (W_n)_{h_1}||W_n \cap (W_n)_{h_2}| > 0$. Then, referring to the set-up in Section 4 in the main document, by the fourth order Campbell formula,

$$
\begin{aligned}
&\mathbb{E}\left\{ \sum_{u,v,u',v' \in X_{W_n}}^{\neq} \frac{f(v-u, v'-u')}{\rho(u)\rho(v)\rho(u')\rho(v')|W_n \cap (W_n)_{v-u}||W_n \cap (W_n)_{v'-u'}|} \right\} \\
&\quad = \int_{W_n^4} \frac{f(v-u, v'-u')}{|W_n \cap (W_n)_{v-u}||W_n \cap (W_n)_{v'-u'}|} \\
&\qquad\qquad g^{(4)}(v-u, u'-u, v'-u)\mathrm{d}u\mathrm{d}v\mathrm{d}u'\mathrm{d}v' \\
&\quad = \int_{(\mathbb{R}^d)^4} f(h_1, h_2) g^{(4)}(h_1, u'-u, h_2+u'-u) \\
&\qquad\qquad \frac{\mathbb{I}\big\{u \in W_n \cap (W_n)_{h_1}, u' \in W_n \cap (W_n)_{h_2}\big\}}{|W_n \cap (W_n)_{h_1}||W_n \cap (W_n)_{h_2}|} \mathrm{d}u\mathrm{d}h_1\mathrm{d}u'\mathrm{d}h_2 \\
&\quad = \int_{\mathbb{R}^d} \int_{\mathbb{R}^d} f(h_1, h_2) \\
&\quad \left\{ \frac{\int_{W_n \cap (W_n)_{h_1}} \int_{W_n \cap (W_n)_{h_2}} g^{(4)}(h_1, u'-u, h_2+u'-u)\mathrm{d}u\mathrm{d}u'}{|W_n \cap (W_n)_{h_1}||W_n \cap (W_n)_{h_2}|} \right\} \mathrm{d}h_1\mathrm{d}h_2.
\end{aligned}
$$

This expectation is the sum of

$$
\begin{aligned}
A &= \int_{\mathbb{R}^d} \int_{\mathbb{R}^d} f(h_1, h_2) \left\{ \frac{\int_{W_n \cap (W_n)_{h_1}} \int_{W_n \cap (W_n)_{h_2}} g(h_1)g(h_2)}{|W_n \cap (W_n)_{h_1}||W_n \cap (W_n)_{h_2}|} \mathrm{d}u\mathrm{d}u' \right\} \mathrm{d}h_1\mathrm{d}h_2 \\
&= \int_{\mathbb{R}^d} \int_{\mathbb{R}^d} f(h_1, h_2) g(h_1) g(h_2) \mathrm{d}h_1\mathrm{d}h_2
\end{aligned}
$$

and

$$
\begin{aligned}
B_n = &\int_{\mathbb{R}^d}\int_{\mathbb{R}^d} f(h_1,h_2) \\
&\left[\frac{\int_{W_n\cap(W_n)_{h_1}}\int_{W_n\cap(W_n)_{h_2}}\left\{g^{(4)}(h_1,u'-u,h_2+u'-u)-g(h_1)g(h_2)\right\}\mathrm{d}u\mathrm{d}u'}{|W_n\cap(W_n)_{h_1}||W_n\cap(W_n)_{h_2}|}\right]\mathrm{d}h_1\mathrm{d}h_2 \\
= &\int_{\mathbb{R}^d}\int_{\mathbb{R}^d} f(h_1,h_2)\Bigg[\int_{\mathbb{R}^d}\frac{|W_n\cap(W_n)_{h_1}\cap(W_n)_{h_3}\cap(W_n)_{h_2+h_3}|}{|W_n\cap(W_n)_{h_1}||W_n\cap(W_n)_{h_2}|} \\
&\qquad\left\{g^{(4)}(h_1,h_3,h_2+h_3)-g(h_1)g(h_2)\right\}\mathrm{d}h_3\Bigg]\mathrm{d}h_1\mathrm{d}h_2.
\end{aligned}
$$

We now specialize to $f(h_1,h_2)=f_k(h_1)f_k(h_2)$, where

$$
f_k(h)=\phi_k(\|h\|-r_{\min})w(\|h\|-r_{\min})\mathbb{I}(h\in B^R_{r_{\min}})/(\varsigma_d\|h\|^{d-1}).
$$

Then, by V3,

$$
\begin{aligned}
|B_n|\leq &\int_{B^R_{r_{\min}}}\int_{B^R_{r_{\min}}} f_k(h_1)f_k(h_2)\Bigg[\int_{\mathbb{R}^d}\frac{|W_n\cap(W_n)_{h_1}\cap(W_n)_{h_3}\cap(W_n)_{h_2+h_3}|}{|W_n\cap(W_n)_{h_1}||W_n\cap(W_n)_{h_2}|} \\
&\qquad\left|g^{(4)}(h_1,h_3,h_2+h_3)-g(h_1)g(h_2)\right|\mathrm{d}h_3\Bigg]\mathrm{d}h_1\mathrm{d}h_2 \\
\leq &C_4\int_{B^R_{r_{\min}}}\int_{B^R_{r_{\min}}}\frac{f_k(h_1)f_k(h_2)}{|W_n\cap(W_n)_{h_1}|}\mathrm{d}h_1\mathrm{d}h_2.
\end{aligned}
$$

Thus B_n tends to zero as $n\to\infty$. Regarding A, we have

$$
\begin{aligned}
A = &\int_{\mathbb{R}^d}\int_{\mathbb{R}^d} f_k(h_1)f_k(h_2)g(h_1)g(h_2)\mathrm{d}h_1\mathrm{d}h_2 \\
= &\left\{\int_{\mathbb{R}^d} f_k(h)g(h)\mathrm{d}h\right\}^2=\left\{\int_{r_{\min}}^{r_{\min}+R} g(r)\phi_k(r-r_{\min})w(r-r_{\min})\mathrm{d}r\right\}^2=\theta_k^2.
\end{aligned}
$$

S2.3 Proof of Theorem 1

We verify that the mean integrated squared error of $\hat{g}_{o,n}$ tends to zero as $n \to \infty$. By (3.7), $\text{MISE}\big(\hat{g}_{o,n}, w\big)/\varsigma_d = \sum_{k=1}^{\infty} \big[b_k(\psi_n)^2\, \mathbb{V}\text{ar}(\hat{\theta}_{k,n}) + \theta_k^2\{b_k(\psi_n)-1\}^2\big]$. By Lemma 1 and condition S1 the right hand side is bounded by

$$BC_1|W_n|^{-1}\sum_{k=1}^{\infty}\big|b_k(\psi_n)\big| + \max_{1\le k\le m}\theta_k^2\sum_{k=1}^{m}(b_k(\psi_n)-1)^2 + (B^2+1)\sum_{k=m+1}^{\infty}\theta_k^2.$$

By Parseval's identity, $\sum_{k=1}^{\infty}\theta_k^2 < \infty$. The last term can thus be made arbitrarily small by choosing m large enough. It also follows that θ_k^2 tends to zero as $k \to \infty$. Hence, by S2, the middle term can be made arbitrarily small by choosing n large enough for any choice of m. Finally, the first term can be made arbitrarily small by S3 and by choosing n large enough.

S2.4 Proof of Theorem 2

Let for $t = (t_1, \ldots, t_d) \in \mathbb{Z}^d$,

$$\Delta(t) = \times_{i=1}^{d}\left(s(t_i - 1/2), s(t_i + 1/2)\right]$$

be the hyper-square with side length s and centered at st. Then, $\{\Delta(t) : t \in \mathbb{Z}^d\}$ is a partition of $\mathbb{R}^d$; i.e., $\Delta(t_1) \cap \Delta(t_2) = \emptyset$ for $t_1 \neq t_2$ and $\cup_{t\in\mathbb{Z}^d}\Delta(t) = \mathbb{R}^d$, and $\big|\Delta_n(t) \oplus R\big| = (s+2R)^d$, where

$$\Delta(t) \oplus R = \times_{i=1}^{d}\left(s(t_i - 1/2) - R, s(t_i + 1/2) + R\right].$$

Let $\mathcal{T}_n = \{t \in \mathbb{Z}^d : \Delta(t) \cap W_n \neq \emptyset\}$ and define

$$Y_n(t) = \sum_{u \in X \cap \Delta(t)} \sum_{\substack{v \in X \setminus \{u\} \\ v-u \in B^R_{r_{\min}}}} \frac{f_n(v-u)\mathbb{I}(u \in W_n, v \in W_n)}{\rho(u)\rho(v)e_n(v-u)}.$$

Then, since $X = \bigcup_{t \in \mathbb{Z}^d} \big(X \cap \Delta(t)\big)$,

$$\begin{aligned} S_n &= \frac{1}{\varsigma_d |W_n|} \sum_{\substack{u,v \in X_{W_n} \\ v-u \in B^R_{r_{\min}}}}^{\neq} \frac{f_n(v-u)}{\rho(u)\rho(v)e_n(v-u)} \\ &= \frac{1}{\varsigma_d |W_n|} \sum_{t \in \mathbb{Z}^d} \sum_{u \in X \cap \Delta(t)} \sum_{\substack{v \in X \setminus \{u\} \\ v-u \in B^R_{r_{\min}}}} \frac{f_n(v-u)\mathbb{I}(u \in W_n, v \in W_n)}{\rho(u)\rho(v)e_n(v-u)} \\ &= \frac{1}{\varsigma_d |W_n|} \sum_{\substack{t \in \mathbb{Z}^d \\ \Delta(t) \cap W_n \neq \emptyset}} Y_n(t) = \frac{1}{\varsigma_d |W_n|} \sum_{t \in \mathcal{T}_n} Y_n(t). \end{aligned}$$

Due to V1, N4 and since $e_n(h) > 1/2^d$ for n large enough and $h \in B^R_{r_{\min}}$,

$$\mathbb{E}(|Y_n(t)|^{2+\lceil \eta \rceil}) \leq \mathbb{E} \left(\sum_{u \in X \cap \Delta(t)} \sum_{\substack{v \in X \setminus \{u\} \\ v-u \in B^R_{r_{\min}}}} \frac{L_2 2^d}{\rho^2_{\min}} \right)^{2+\lceil \eta \rceil}.$$

The moments $\mathbb{E}(|Y_n(t)|^{2+\lceil \eta \rceil})$ are thus bounded by sums of integrals involving $g^{(k)}(u_1, \ldots, u_{k-1})$ times $(L_2 2^d/\rho^2_{\min})^{2+\lceil \eta \rceil}$ for $k = 2, \ldots, 2(2+\lceil \eta \rceil)$. These integrals are bounded uniformly in t and n due to assumption N2. Thus,

$$\sup_{n \geq 1} \sup_{t \in \mathcal{T}_n} \mathbb{E}(|Y_n(t)|^{2+\eta}) \leq \sup_{n \geq 1} \sup_{t \in \mathcal{T}_n} \mathbb{E}(|Y_n(t)|^{2+\lceil \eta \rceil}) < \infty$$

and hence $\{|Y_n(t)|^{2+\eta} : t \in \mathcal{T}_n, n \geq 1\}$ is a uniformly integrable family (triangular array) of random variables. Invoking finally N1 and N3 and letting $\sigma_n^2 = \mathbb{V}\mathrm{ar}\{\sum_{t\in\mathcal{T}_n} Y_n(t)\}$, it follows directly from Theorem 3.1 in Biscio and Waagepetersen (2016) that

$$\sigma_n^{-1} \sum_{t\in\mathcal{T}_n} \left[Y_n(t) - \mathbb{E}\{Y_n(t)\}\right] \xrightarrow{D} N(0,1),$$

which is equivalent to Theorem 2.

S3 Order of sum of products of Bessel basis functions

In this section we consider the Fourier-Bessel basis in the case $r_{\min} = 0$. It is known (see Watson, 1995, p. 199) that as $r \to \infty$,

$$J_\nu(r) \sim \left(\frac{2}{\pi r}\right)^{1/2} \cos\left(r - \frac{\nu\pi}{2} - \frac{\pi}{4}\right),$$

which implies that

$$\alpha_{\nu,k} = (k + \frac{\nu}{2} - \frac{1}{4})\pi + O(k^{-1}), \quad \text{as } k \to \infty, \tag{S3.4}$$

and $\alpha_{\nu,k} \to \infty$, as $k \to \infty$. We can argue that for large k,

$$\begin{aligned} J_{\nu+1}(\alpha_{\nu,k}) &\approx \left(\frac{2}{\pi\alpha_{\nu,k}}\right)^{1/2} \cos\left(\alpha_{\nu,k} - \frac{\pi}{4} - \frac{(\nu+1)\pi}{2}\right) \\ &= \left(\frac{2}{\pi\alpha_{\nu,k}}\right)^{1/2} \cos\left((k-1)\pi + O(k^{-1})\right), \end{aligned}$$

and consequently

$$\left|J_{\nu+1}(\alpha_{\nu,k})\right| \approx \left(\frac{2}{\pi\alpha_{\nu,k}}\right)^{1/2}. \tag{S3.5}$$

On the other hand, for $\nu \geq 0$ and $r > 0$ (Landau, 2000),

$$\left|J_\nu(r)\right| \leq \frac{c}{|r|^{1/3}},$$

where $c = 0.7857468704\ldots$, and hence

$$\left|\phi_k(r)\right| \le \frac{cr^{-\nu-1/3}\sqrt{2}}{(R^2\alpha_{\nu,k})^{1/3}\left|J_{\nu+1}(\alpha_{\nu,k})\right|} \quad r > 0, k \ge 1.$$

Using (S3.4) and (S3.5), for large k,

$$\frac{cr^{-\nu-1/3}\sqrt{2}}{(R^2\alpha_{\nu,k})^{1/3}\left|J_{\nu+1}(\alpha_{\nu,k})\right|} \approx c\sqrt{\pi}\frac{r^{-\nu-1/3}}{R^{2/3}}\alpha_{\nu,k}^{1/6} \approx c\sqrt{\pi}\frac{r^{-\nu-1/3}}{R^{2/3}}\big\{(k+\frac{\nu}{2}-\frac{1}{4})\pi\big\}^{1/6}.$$

Since $\lim_{r\to 0} J_\nu(r)r^{-\nu} = \{\Gamma(\nu+1)2^\nu\}^{-1}$, we also obtain for large k and $0 < \|h\| < R$,

$$|\phi(\|h\|)| \le \text{const}\left(\frac{R}{\alpha_{\nu,k}}\right)^{-\nu}\frac{\sqrt{2}}{RJ_{\nu+1}(\alpha_{\nu,k})} \approx \text{const}\sqrt{\pi}\frac{\alpha_{\nu,k}^{\nu+1/2}}{R^{\nu+1}} = O(k^{\nu+1/2}).$$

Thus, for fixed r and $0 < \|h\| < R$,

$$|\phi_k(r)\phi_k(\|h\|)| = O(k^{1/6+\max(1/6,\nu+1/2)}) = O(k^{1/6+\max(1/6,d/2-1/2)}).$$

By generalization of Faulhaber's formula (McGown and Parks, 2007),

$$\sum_{k=1}^{K_n} k^p = O(K_n^{p+1}), \quad p > -1.$$

Therefore,

$$\frac{1}{K_n^\omega}\sum_{k=1}^{K_n}\left|\phi_k(r)\phi_k(\|h\|)\right| = \begin{cases} O(K_n^{4/3-\omega}) & d = 1 \\ O(K_n^{d/2+2/3-\omega}) & d > 1 \end{cases}$$

for $\omega > 0$ and $0 < r, \|h\| < R$.

S4 Simulation study

The results in Figure S1 are obtained as for the simulation study in the main document but with $W = [0, 2]^2$. The estimated cut-offs $\hat{K}$ are summarized in Table S1. Simulation mean and 95% envelopes for $\hat{g}_k$, $\hat{g}_c$ and $\hat{g}_o$ with both Fourier-Bessel and cosine basis and simple smoothing schemes are shown for $W = [0, 2]^2$ in Figure S2. Figure S3 shows histograms of orthogonal series estimates. Comments on these figures and the table are given in the main document.

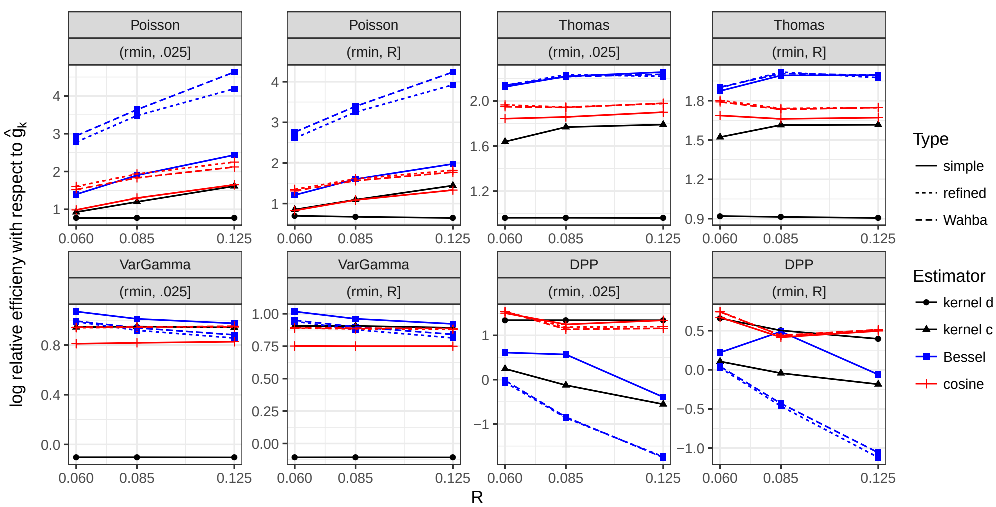

Figure S1: Plots of log relative efficiencies for small lags $(r_{\min}, 0.025]$ and all lags $(r_{\min}, R]$, $R = 0.06, 0.085, 0.125$, and $W = [0, 2]^2$. Black: kernel estimators. Blue and red: orthogonal series estimators with Bessel respectively cosine basis. Lines serve to ease visual interpretation.

S5 Data example

Figure S4 shows the data sets and fitted intensity functions considered in Section 7 of the main document. For the *Capparis frondosa* species and the orthogonal series estimator with cosine basis, the function $\hat{I}(K)$ given in (5.14) of the main document is shown in Figure S5. Although $\hat{I}(K)$ is decreasing over $1 \leq K \leq 49$, the rate of decrease slows down after $K = 7$.

S6 Behavior of the Fourier-Bessel and cosine basis

Figure S6 shows the Fourier-Bessel and cosine basis functions $\phi_k(r)$ in the planar case ($d = 2$) for $R = 0.125$, $k = 1, \ldots, 8$ and $r \in [0, 0.125]$. Obviously, the cosine basis functions are uniformly bounded and integrable. However, the Fourier-Bessel basis functions exhibit damped oscillation behavior with $\phi_k(R) = 0$ and

$$\phi_k(0) = \frac{\alpha_{\nu,k}^{\nu}}{R^{\nu+1} 2^{\nu-1/2} \Gamma(\nu+1) J_{\nu+1}(\alpha_{\nu,k})},$$

for all $k \geq 1$, because $\lim_{r \to 0} J_\nu(r) r^{-\nu} = 1/(\Gamma(\nu+1)2^\nu)$ for $\nu \geq 0$. Thus, $\phi_k(0) \to \infty$ as $k \to \infty$.

For $0 \leq \nu \leq 1/2$ (or equivalently $d = 2, 3$), $|J_\nu(r)| \leq (2/\pi r)^{1/2}$ and hence

$$\int_0^{\alpha_{\nu,k}} \big|J_\nu(r)\big| r^{\nu+1} \mathrm{d}r \leq \left(\frac{2}{\pi}\right)^{1/2} \int_0^{\alpha_{\nu,k}} r^{\nu+\frac{1}{2}} \mathrm{d}r = \left(\frac{2}{\pi}\right)^{1/2} \frac{(\alpha_{\nu,k})^{\nu+\frac{3}{2}}}{\nu+\frac{3}{2}}.$$

Therefore, as $k \to \infty$,

$$\begin{aligned}
\int_0^R \big|\phi_k(r)\big| w(r)\mathrm{d}r &= \frac{\sqrt{2}}{R\big|J_{\nu+1}(\alpha_{\nu,k})\big|}\left(\frac{R}{\alpha_{\nu,k}}\right)^{\nu+2}\int_0^{\alpha_{\nu,k}} \big|J_\nu(r)\big| r^{\nu+1}\mathrm{d}r \\
&\le \frac{\sqrt{2}}{R\big|J_{\nu+1}(\alpha_{\nu,k})\big|}\left(\frac{R}{\alpha_{\nu,k}}\right)^{\nu+2}\left(\frac{2}{\pi}\right)^{1/2}\frac{(\alpha_{\nu,k})^{\nu+\frac{3}{2}}}{\nu+\frac{3}{2}} \\
&= \frac{2R^{\nu+1}}{\big|J_{\nu+1}(\alpha_{\nu,k})\big|(\pi\alpha_{\nu,k})^{1/2}(\nu+\frac{3}{2})} \\
&\approx \frac{2R^{\nu+1}}{(\frac{2}{\pi\alpha_{\nu,k}})^{1/2}(\pi\alpha_{\nu,k})^{1/2}(\nu+\frac{3}{2})} = \frac{\sqrt{2}R^{\nu+1}}{\nu+\frac{3}{2}} < \infty,
\end{aligned}$$

which implies uniform integrability of $\phi_k(r)$.

Bibliography

Biscio, C. A. N. and Waagepetersen, R. (2016). A central limit theorem for α-mixing spatial point processes. Manuscript.

Landau, L. (2000). Monotonicity and bounds on Bessel functions. In *Proceedings of the Symposium on Mathematical Physics and Quantum Field Theory*, volume 4, pages 147–154. Southwest Texas State Univ. San Marcos, TX.

McGown, K. J. and Parks, H. R. (2007). The generalization of Faulhaber's formula to sums of non-integral powers. *Journal of Mathematical Analysis and Applications*, 330(1):571 – 575.

Møller, J. and Waagepetersen, R. P. (2003). *Statistical inference and simulation for spatial point processes*. Chapman and Hall/CRC, Boca Raton.

Watson, G. N. (1995). *A treatise on the theory of Bessel functions*. Cambridge university press.

Table S1: Monte Carlo mean and quantiles of the estimated cut-off $\hat{K}$ obtained from (5.15) for the orthogonal series estimator with Fourier-Bessel (FB) and cosine (CO) bases and their ratio (CO/FB) in the case of Poisson (P), Thomas (T), Variance Gamma (V) and determinantal (D) point processes on observation windows $W_1 = [0,1]^2$ and $W_2 = [0,2]^2$ with $r_{\min} = 0.001$.

			$R = 0.06$			$R = 0.085$			$R = 0.125$		
			$\hat{\mathbb{E}}(\hat{K})$	$\hat{q}_{0.05}(\hat{K})$	$\hat{q}_{0.95}(\hat{K})$	$\hat{\mathbb{E}}(\hat{K})$	$\hat{q}_{0.05}(\hat{K})$	$\hat{q}_{0.95}(\hat{K})$	$\hat{\mathbb{E}}(\hat{K})$	$\hat{q}_{0.05}(\hat{K})$	$\hat{q}_{0.95}(\hat{K})$
W_1	P	FB	2.17	2.00	3.00	2.15	2.00	3.00	2.11	2.00	3.00
		CO	2.31	2.00	4.00	2.35	2.00	4.00	2.34	2.00	4.00
		CO/FB	1.08	0.67	1.50	1.10	1.00	1.67	1.12	1.00	2.00
	T	FB	2.24	2.00	3.00	2.24	2.00	3.00	3.23	2.00	4.05
		CO	2.39	2.00	4.00	2.52	2.00	4.00	3.54	3.00	5.00
		CO/FB	1.10	0.67	2.00	1.16	0.67	1.50	1.14	0.75	1.76
	V	FB	2.77	2.00	4.00	3.50	2.00	6.00	4.85	3.00	8.00
		CO	3.06	2.00	5.00	4.17	2.00	7.00	5.78	3.00	10.00
		CO/FB	1.14	0.67	2.00	1.26	0.75	2.33	1.27	0.75	2.50
	D	FB	2.21	2.00	3.00	2.18	2.00	3.00	2.38	2.00	3.00
		CO	2.23	2.00	3.00	2.46	2.00	4.00	3.30	2.00	5.00
		CO/FB	1.04	0.67	1.50	1.15	1.00	1.50	1.45	1.00	2.00
W_2	P	FB	2.17	2.00	3.00	2.12	2.00	3.00	2.09	2.00	3.00
		CO	2.34	2.00	4.00	2.32	2.00	4.00	2.36	2.00	4.00
		CO/FB	1.10	0.67	2.00	1.11	0.67	2.00	1.13	1.00	2.00
	T	FB	2.39	2.00	4.00	2.46	2.00	4.00	3.78	3.00	5.00
		CO	2.43	2.00	5.00	3.17	2.00	5.00	4.19	3.00	6.00
		CO/FB	1.08	0.50	2.50	1.35	1.00	2.00	1.13	0.75	1.67
	V	FB	3.58	3.00	5.00	5.14	3.00	8.00	7.19	5.00	11.00
		CO	4.76	3.00	9.00	6.40	4.00	12.00	9.03	5.00	17.00
		CO/FB	1.38	0.80	2.67	1.30	0.80	2.56	1.30	0.83	2.43
	D	FB	2.22	2.00	4.00	2.17	2.00	3.00	2.79	2.00	4.00
		CO	2.19	2.00	3.00	2.92	2.00	4.00	3.74	3.00	5.00
		CO/FB	1.02	0.67	1.50	1.38	1.00	2.00	1.40	1.00	2.00

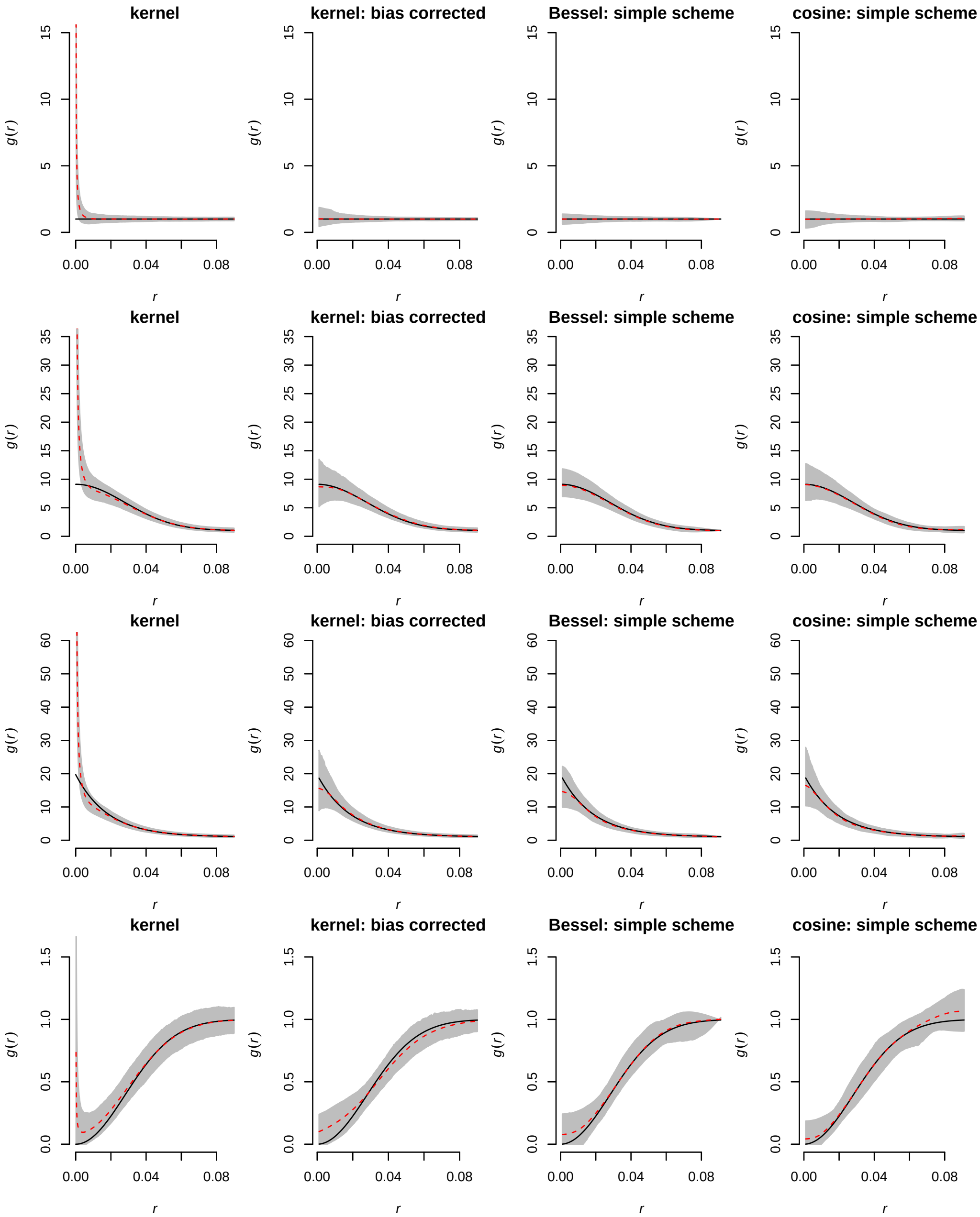

Figure S2: True pair correlation function (solid line), Monte Carlo mean (dashed lines) and 95% pointwise probability interval (grey area) of estimates based on $n_{\text{sim}} = 1000$ simulations from the Poisson (first row), Thomas (second row), Variance Gamma (third row) and determinantal (fourth row) point processes on $W = [0, 2]^2$.

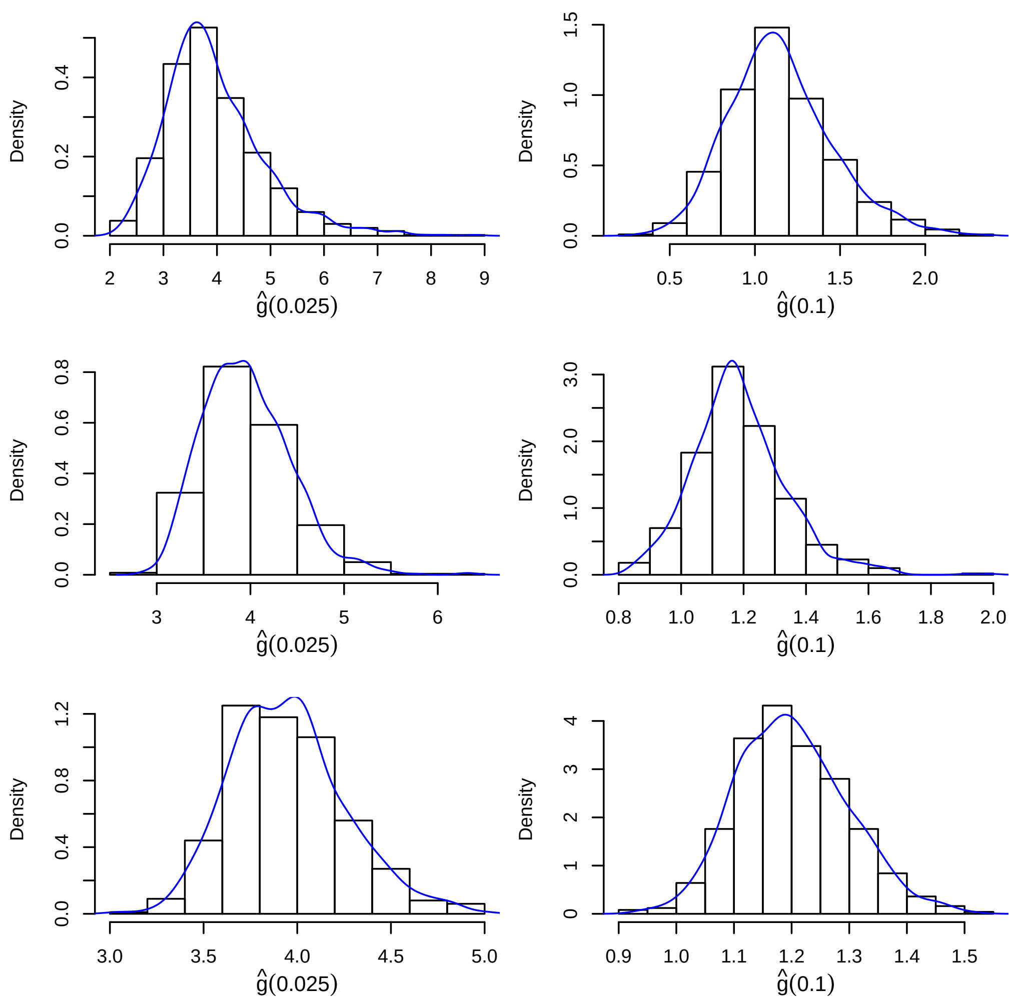

Figure S3: Histograms of $\hat{g}_o(r)$ at $r = 0.025$ and $r = 0.1$ using the Bessel basis with the simple smoothing scheme in case of the Thomas process on $W = [0,1]^2$ (upper panels), $W = [0,2]^2$ (middle panels) and $W = [0,3]^2$ (lower panels).

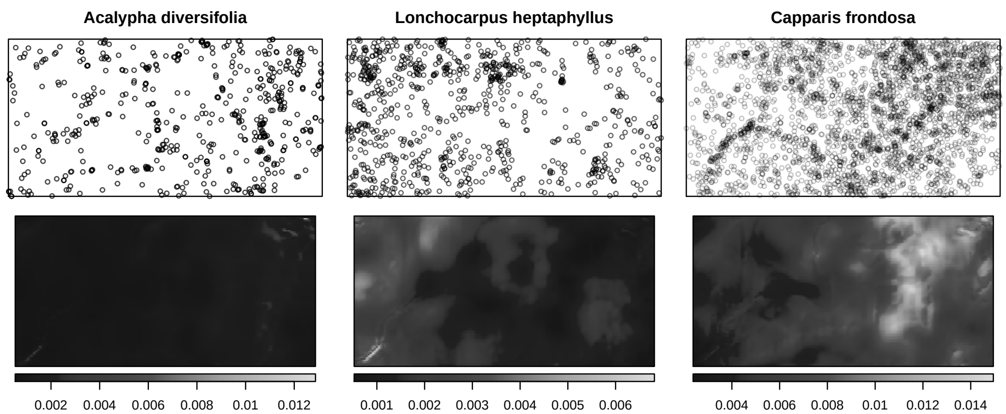

Figure S4: Locations of *Acalypha diversifolia*, *Lonchocarpus heptaphyllus* and *Capparis frondosa* trees in the Barro Colorado Island plot (upper panels) and their fitted parametric intensity functions (lower panels).

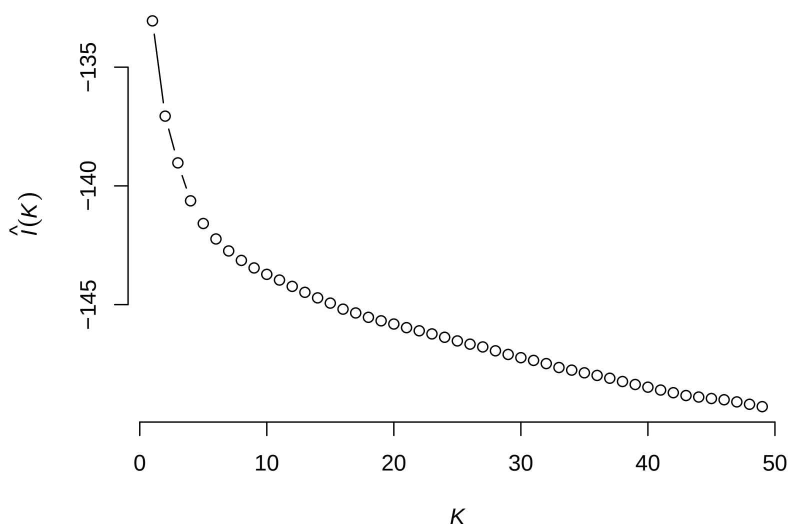

Figure S5: Estimate $\hat{I}(K)$ of the mean integrated squared error for *Capparis frondosa* in case of the orthogonal series estimator with cosine basis.

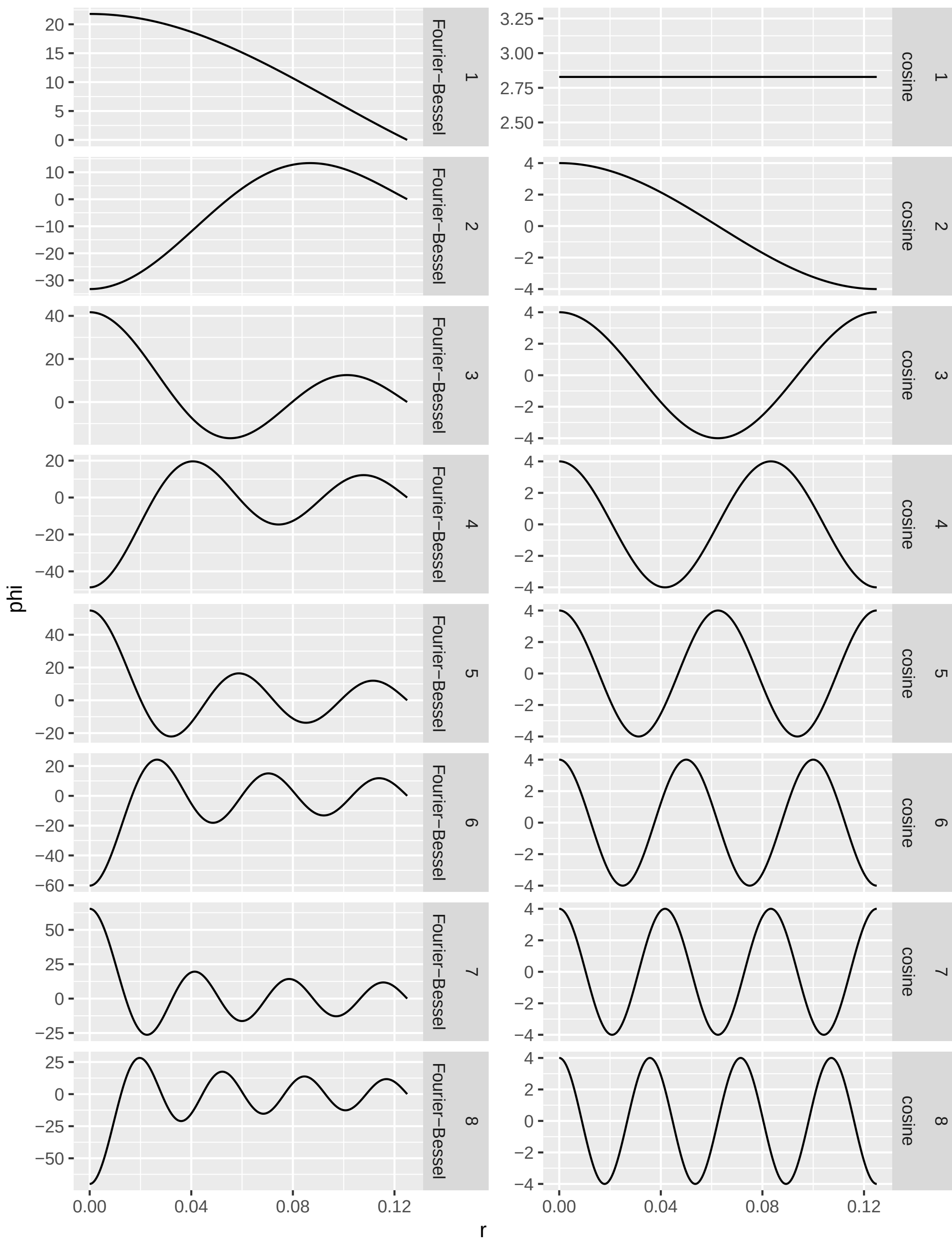

Figure S6: Fourier-Bessel and cosine basis functions $\phi_k(r)$ in the planar case ($d = 2$) for $R = 0.125$ and $k = 1, \ldots, 8$.